

**ASAS Photometry of ROSAT Sources.
II. New Variables from the ASAS North Survey**

M. Kiraga and K. Stępień

Warsaw University Observatory, Al. Ujazdowskie 4, 00-478 Warsaw, Poland
e-mail: (kiraga,kst)@astrouw.edu.pl

Received January 22, 2013

ABSTRACT

We present a catalog of 307 optical counterparts of the bright ROSAT X-ray sources, identified with the ASAS North survey data and showing periodic brightness variations. They all have declination north of -25° . Other data available from the literature for the listed stars are also included. All the tabulated stars are new variables, except for 13 previously known, for which the revised values of periods are given.

Key words: *Stars: variables: general – Stars: rotation – Stars: activity – X-rays: stars*

1. Introduction

Coronal-chromospheric activity is common among cool stars possessing sub-photospheric convection zones (Wilson 1963, Pallavicini *et al.* 1981). Its ubiquitous presence in these stars finds a support in theoretical considerations, according to which the presence of a convective layer in a rotating body is sufficient for development of the dynamo mechanism efficiently strengthening even a very weak, “seed” magnetic field (Parker 1955). The field is most likely generated at the interface between the convection zone and the radiative core or, possibly, in the bulk of the convective layer. Due to buoyancy, magnetic tubes are brought to stellar surface where they interact with convection, producing several phenomena known under the collective name of activity. Observations and theory show that the stellar activity level depends on the internal structure of a star and its rotation rate (Durney and Latour 1978, Noyes *et al.* 1984). In particular, rapidly rotating cool stars show high levels of activity as measured by strong surface magnetic fields, intense chromospheric and coronal emission, and appearance of the numerous cool star spots believed to be regions of the high concentration of the local magnetic field. As the observations of cool stars (including our Sun) show, the spots are often distributed nonuniformly over the stellar surface, hence rotational modulation of the star’s brightness is expected. Systematic photometry of a large number of

active stars makes possible the detection of this modulation and determination of the stellar rotation period – a crucial parameter for analyzing the activity level, and its dependence on global stellar parameters such as mass, age, evolutionary stage or chemical composition. Ideal for this purpose are photometric surveys covering a large part of the sky. One of these is ASAS (Pojmański 1997, 2004). It began twelve years ago on the Southern hemisphere (ASAS-S) while its Northern twin (ASAS-N) is in operation since 2006.

The analysis of the rotation of main sequence M-type stars, based on the ASAS-S data, was carried out by Kiraga and Stępień (2007). Many new rotation periods were determined, among them a number with the length of several tens of days, which were particularly useful for discussion of the period-activity relation. Later, Kiraga (2012) analyzed all stars from the ASAS-S survey for which the X-ray flux could be found in the ROSAT Bright Source Catalog (RBSC) from the ROSAT All Sky Survey. The ASAS-S photometry is available for stars with declination up to $+29^\circ$. Kiraga (2012) identified 6028 such stars. Among them 2302 stars showed periodic variability. An extensive catalog was prepared where all the periodic variables are listed, together with the data on their variability type and other interesting information available from the literature.

The present paper is a continuation of the investigation by Kiraga (2012). We repeat the same procedure for the Northern ROSAT bright sources and photometric observations from the ASAS-N survey as Kiraga (2012) did for the Southern hemisphere.

2. X-Ray and Photometric Observations and Data Analysis

The ROSAT All Sky Survey was obtained between July 30, 1990 and January 25, 1991, with additional observations taken in February and August 1991 (Voges *et al.* 1999). Analysis of the survey data resulted in the detection of 145 060 sources. Among them 18 811 sources were classified as “bright” and published by Voges *et al.* (1999) in RBSC. A source was classified as bright when its count rate was higher than 0.05 cts/s in the 0.1–2.4 keV energy band and at least 15 photon counts were registered.

The ASAS-N station is located at Haleakala (Maui, Hawaii Islands). The photometric survey is carried out using the Nikkor 200mm f/2.0 lens equipped with the Apogee AP-10, 2048×2048 CCD camera which has the angular resolution of 15 arcsec/pixel. We used only the V-band data in the present analysis, taken between May 29, 2006 and February 12, 2012 for stars with declination north of -25° . We decided to include into our analysis also stars from the equatorial belt (with declination between -25° and $+29^\circ$) which had already been investigated by Kiraga (2012). We did so because ASAS-N has a larger aperture, hence useful data are available for stars fainter than from ASAS-S. Furthermore, ASAS-S stopped collecting data in October 2008 due to some problems with the new CCD

cameras so the data obtained later by ASAS-N may be used for variability search of previously non detected variables.

There are 12 910 entries in the RBSC located north of declination -25° . The optical identification of the X-ray sources was based on the coordinates of the X-ray sources given in the ROSAT catalog. Using the ASAS photometric database we searched for an optical counterpart within $30''$ from each RBSC source. The distance of $30''$ corresponds approximately to two ASAS pixels. We restricted our attention only to stars with the mean V brightness between 8 mag and 14.0 mag for which at least 40 observations are available, so a reasonable period analysis can be performed.

We identified 4324 stars fulfilling the above criteria. A preliminary period search was done with the AOV algorithm developed and described by Schwarzenberg-Czerny (1989). Because many stars show season to season variations, usually interpreted as resulting from the long term activity cycles, we carried out the period search separately for each season, unless the number of useful observations in the particular season was lower than 40. A period search was also done on the whole data set after shifting the individual seasonal means to the common level. The data points deviating by more than 3.5 standard deviations from the seasonal mean were treated as outliers and rejected (Kiraga and Stępień 2007).

Using 6 phase bins, we obtained the value of the AOV statistics higher than 10 for 1603 stars, of which 647 have already been listed in Kiraga (2012). The latter stars were excluded from the further analysis. Although the majority of the presently obtained periods are in agreement with the old ones, several new periods differ substantially, *e.g.*, by a factor of two, or are related to one another as 1 d aliases. There are, however, stars for which new periods are not apparently related to the old ones. Detailed comparison of the new and old periods as well as a discussion of all detected variables in the equatorial belt covered by both ASAS surveys will be presented in the forthcoming paper.

Of the remaining 956 objects, 37 were found in the ASAS catalog ACVS and additional 159 stars were listed in the catalogs by Norton *et al.* (2007), Hartman *et al.* (2011) and Pigulski *et al.* (2009). So, after the first step, we were left with 760 suspected periodic variables. In the second step, we applied the CLEAN algorithm (Roberts *et al.* 1987) to each data set and, in addition, we critically inspected the resulting photometric curves visually. Many of the stars which had passed the CLEAN test, are marked as variables in the SIMBAD database. They were also removed from our sample, unless a new or revised value of the period was obtained with a high level of confidence (see below). As a final step, we formed a list of 307 objects with definitely present periodic variability.

Although the approximate estimate indicates that out of 4000 coincidences between X-ray and ASAS sources about 0.5% may be spurious, the probability of a spurious coincidence of a variable star and the X-ray source is much lower so we expect that at most one such case occurs among 307 investigated objects.

So far, only V -band ASAS-N photometric data are reduced and released to a public domain. In lack of measurements in another optical band, we used 2MASS photometry (Skrutskie *et al.* 2006) to obtain color information for each investigated star. We adopted the J -band data because a reliable calibration of the bolometric correction based on the $V - J$ color exists for F–M stars (Casagrande *et al.* 2008, 2010). Since 2MASS survey has a substantially better resolution than ASAS ($2.''5$ vs. $15.''$) we had to apply a special procedure to obtain a reliable J magnitude related to our optical object. Low resolution of the ASAS survey means that fluxes from all sources lying closer than about $30.''$ from the optically identified object add to its V measurement. To apply a respective correction to the J data, we counted all the 2MASS sources within $40.''$ (with allowance for the additional margin of $10.''$) from the position of the ASAS source and added together their J fluxes. The brightest source was assumed to correspond to the optical object but its J brightness was corrected by adding to it the fluxes of all the counted nearby sources. The directly measured J magnitude of the brightest source is listed in our catalog, together with the relative total J flux of all the counted sources, expressed in units of the brightest source flux. A relative total flux like 1.04 means that the adopted J flux of the brightest source was corrected by 4% before forming a color index $V - J$. As it is seen from the catalog, the relative total flux does not exceed 1.05 in most cases but it can reach a value of 2 or more for a star with nearby companion(s) of a comparable brightness. The total flux expressed in magnitudes is listed as J_{cor} . This flux was used together with the V -magnitude to calculate the bolometric correction of each identified star. For stars with $(V - J_{\text{cor}}) < 2.4$ mag the formula given by Casagrande *et al.* (2010) was used (where F_{bol} is expressed in $\text{erg cm}^{-2} \text{s}^{-1}$):

$$\log(F_{\text{bol}}) = -0.4 \cdot J + \log(fc) - 5$$

where

$$fc = 2.7915 - 2.8096 \cdot (V - J_{\text{cor}}) + 1.2799 \cdot (V - J_{\text{cor}})^2 - 0.2049 \cdot (V - J_{\text{cor}})^3.$$

For stars with $(V - J_{\text{cor}}) > 2.4$ mag we used the second order formula obtained from the fitting to the data given by Casagrande *et al.* (2008):

$$BC_J = 0.8439 + 0.3652 \cdot (V - J_{\text{cor}}) - 0.0267 \cdot (V - J_{\text{cor}})^2,$$

$$m_{\text{bol}} = J + BC_{J_{\text{cor}}},$$

and

$$\log(F_{\text{bol}}) = -0.4 \cdot (m_{\text{bol}} - 4.75) - 6.489.$$

The uncertainty of the bolometric flux is dominated by the uncertainty of the J and J_{cor} because it is based on a single measurement taken at a random phase of the variability period. We assume that it is equal to the standard deviation of the V measurement for each star *i.e.*, σ_V . Other uncertainties, like the error of $\langle V \rangle$, or

calibration errors are significantly lower. According to our estimate, the error of $\log(F_{\text{bol}})$ does not exceed 0.05 (but see below).

The X-ray flux in the 0.1–2.4 keV range was calculated from the data given in RBSC using a formula provided by Fleming *et al.* (1995):

$$F_x = (5.31HR1 + 8.31) \cdot 10^{-12} \text{ cts}$$

where *HR1* is the hardness ratio:

$$HR1 = (B - A)/(A + B)$$

with *B* – a number of counts in the 0.4–2.0 keV range and *A* – a number of counts in the 0.1–0.4 keV range. Here F_x is expressed in $\text{erg cm}^{-2} \text{ s}^{-1}$ and “cts” means counts per second.

From F_x and F_{bol} the ratio $R_x = \log(F_x/F_{\text{bol}})$ was calculated for each variable. The error of R_x is dominated by the error of the X-ray measurement. It is listed in the catalog along with the value of R_x . However, for stars with large relative total fluxes, the J_{cor} -value, hence $\log(F_{\text{bol}})$, may be erroneous, due to a possible misidentification of the optical source or the presence of the nearby, bright infrared source. So, the values of R_x for stars with the relative total flux exceeding, say, 1.25 should be treated with caution.

3. New Variable Stars

3.1. Properties of New Variables

In this section we briefly summarize the basic properties of the new variable stars. We also call attention to several individual stars with particularly interesting properties.

Most of the investigated stars have so far not been extensively observed so very limited data on them can be found in the SIMBAD database. Spectral types are known only for 136 stars, parallaxes have been measured for 17, and radial velocity for mere 19 objects. Among those with known spectral classification there are two A-type, 12 F-type, 35 G-type, 73 K-type and 14 M-type stars.

The classification of the variability type of the new variables was based on the visually identified characteristic features of their light curves, and on the level of X-ray emission relative to the bolometric flux. As a result, 266 stars were classified as spotted rotators, although a low amplitude variation in some of them makes difficult to distinguish a spotted variable from an ellipsoidal, or tidally deformed object. Among other variables 10 contact binaries were identified, 12 eclipsing binaries with deformed components but not in contact and 18 detached eclipsing binaries. One optical counterpart (ASAS 071404+7004.3) to the X-ray source 1RXS J071404.0+700413 was classified as a miscellaneous variable.

Fig. 1 presents a few statistical properties of the investigated stars. Fig. 1a gives an apparent magnitude distribution of the new variables. The number of stars

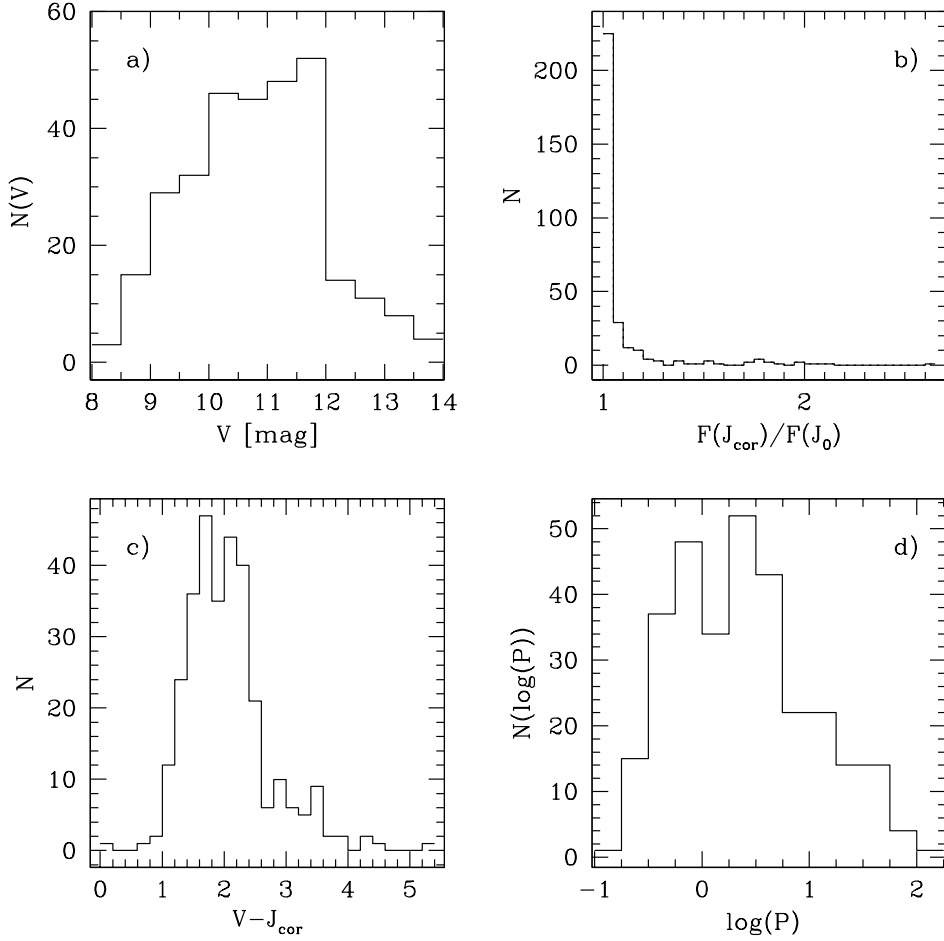


Fig. 1. *a)* Apparent V -distribution of the new variables in 0.5 mag bins. *b)* Histogram of the flux in the J -band from all sources located within $40''$ of ASAS position expressed in the J -band flux from the brightest source (see text). For most stars the contribution to J -band flux from fainter objects is small. *c)* Color index $V - J_{\text{cor}}$ distribution of the new variables in 0.1 mag bin. See text for definition of J_{cor} . *d)* Period distribution of the detected variables. The number of stars is given per 0.25 bin in $\log(P)$ (with period in days).

increases almost linearly between 9 mag and 12 mag and falls off outside of this range. In our sample, there are only three stars brighter than 8.5 mag, of which ASAS 025746+4431.5 (HD 18281) with $V = 8.32$ mag is the brightest, and five stars fainter than 13.5 mag. The histogram representing the number of stars as a function of the relative total flux is presented in Fig. 1b. This flux is lower than 1.05 for 225 stars, and exceeds 1.25 for 27 stars. Among the latter, it is higher than 2.0 for four stars. Fig. 1c shows the color distribution of the variables. Most of them fall within the range $1 < (V - J_{\text{cor}}) < 3$. Only four stars are hotter than that and

28 stars have the color index exceeding 3.0. The period distribution is shown in Fig. 1d. About 90% of stars are in the period range between 0.315 d and 37 d with overall maximum of the period distribution around 2–3 d. Among the short-period variables two have periods shorter than 0.2 d and three have periods between 0.2 d and 0.25 d. In the long-period tail two stars have periods longer than 100 d and four have periods between 50 d and 100 d.

3.2. Comments on a Few Interesting Stars

ASAS 071404+7004.3 is the hottest star in our sample with $(V - J_{\text{cor}}) = 0.09$ mag which seems to rule out the coronal origin of its X-ray flux. This star has also an unusually high X-ray to bolometric flux ratio $R_x = -2.46$, and the light curve very different from other analyzed stars (see Fig. 2). It may be a previously unrecognized cataclysmic variable with a period of 22.4 d.

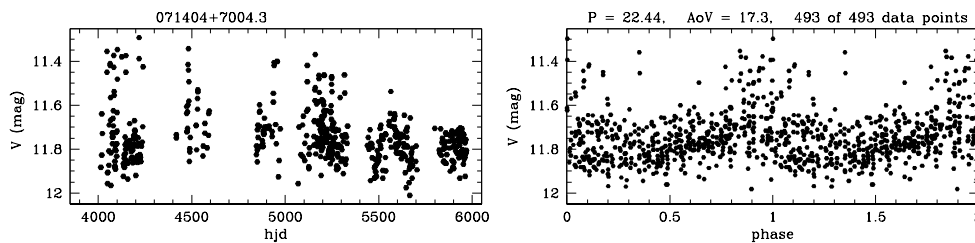


Fig. 2. Photometric data points for ASAS 071404+7004.3 are presented on the *left panel* (as a function of $\text{hjd} = \text{HJD} - 2450000$). Phased light curve of data showing periodic variability is presented on the *right panel*.

ASAS 205846+1417.8 (HD 199742) has the reddest color in our sample, $(V - J_{\text{cor}}) = 5.35$ mag, and has also the highest bolometric luminosity. Its small proper motion suggests that it may be a distant M-type red giant, however, its variability period of only 22 d seems to be too short for the rotational modulation. The star may also be an example of a low amplitude pulsating red giant (Soszyński *et al.* 2011) although these stars are not known to possess active coronae.

ASAS 235257+6250.0 (BD+62 2316) has the shortest period of $P=0.158038$ d. It is classified as a spotted rotator due to its low amplitude and variable light curve. Similarly classified is a star (ASAS 034327+2935.6 = BD+29 599, $P = 0.187213$) with the second shortest period. However, the classification of both stars is very uncertain; they can very well be eclipsing contact (EC) binaries with periods two times longer than adopted here. Two other stars with period shorter than 0.25 d are certain EC binaries (ASAS 040959+5558.9 = BD+55 849 – with $P = 0.242750$ d and ASAS 082931+7231.7 with $P = 0.231400$ d).

ASAS 030755+6031.4, with $P = 0.20629$ d, shows a very peculiar light curve, reminiscent that of a pulsating star with a sharp rise and a gradual decline (see Fig. 3) but we classified it as a rotationally variable due to its X-ray emission typical of the high activity stars.

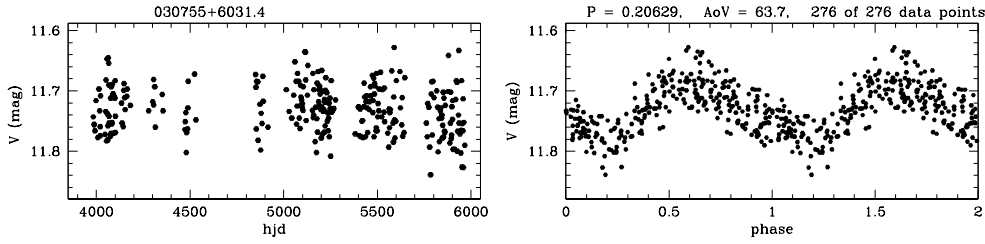


Fig. 3. Photometric data points for ASAS 030755+6031.4 are presented on the *left panel* (as a function of $\text{hjd} = \text{HJD} - 2450000$). Phased light curve of data showing periodic variability is presented on the *right panel*.

Periods of 10 EC binaries are between $P=0.231400$ d (ASAS 082931+7231.7) and $P = 0.376532$ d (ASAS 034501+4937.0). Detached eclipsing (ED) binaries have periods from $P=0.659984$ d (ASAS 141331+2644.8) to $P=3.8581$ d (ASAS 083103+6948.9), whereas the periods of eclipsing β -Lyr type (EB) binaries fall between 0.393273 d (ASAS 061335+4914.1) and 37.685 d (ASAS 224336+4445.1). The latter star is very likely an ED binary with narrow eclipses and strong brightness variations between eclipses due to the presence of spots (see Fig. 4).

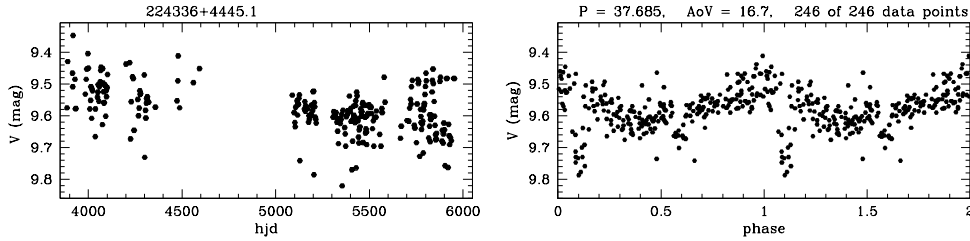


Fig. 4. Photometric data points for ASAS 224336+4445.1 are presented on the *left panel* (as a function of $\text{hjd} = \text{HJD} - 2450000$). Phased light curve of data showing periodic variability is presented on the *right panel*.

All stars with periods above 50 d (ASAS 025412+4035.4 – HD 17930, $P = 100$ d; ASAS 062445+4316.1 – BD+43 1525, $P = 64.8$ d; ASAS 202740+7734.3 – BD+77 779, $P = 56.8$ d; ASAS 203417+3100.6 – HD 334646, $P = 68.9$ d; ASAS 205131+4547.2 – BD+45 3306, $P = 53.8$ d; ASAS 213240+3604.7 – HD 205173, $P = 109.7$ d) have spectral types in the range G5–K2 and proper motions below 31 mas/year. Their R_x values are in the range from -4.3 to -3.6 , and the hardness ratio is above 0.40. All these data suggest that they are active giants.

3.3. Data on the Investigated Variables

The catalog of the 307 periodic variables is given in Table 1. For illustration, we list here the first three entries of the catalog and Fig. 5 shows a few examples of the light curves. Full Table 1 and all light curves are available in the electronic form from the *Acta Astronomica Archive* (ftp://ftp.astro.uw.edu.pl/acta/2013/kir_53).

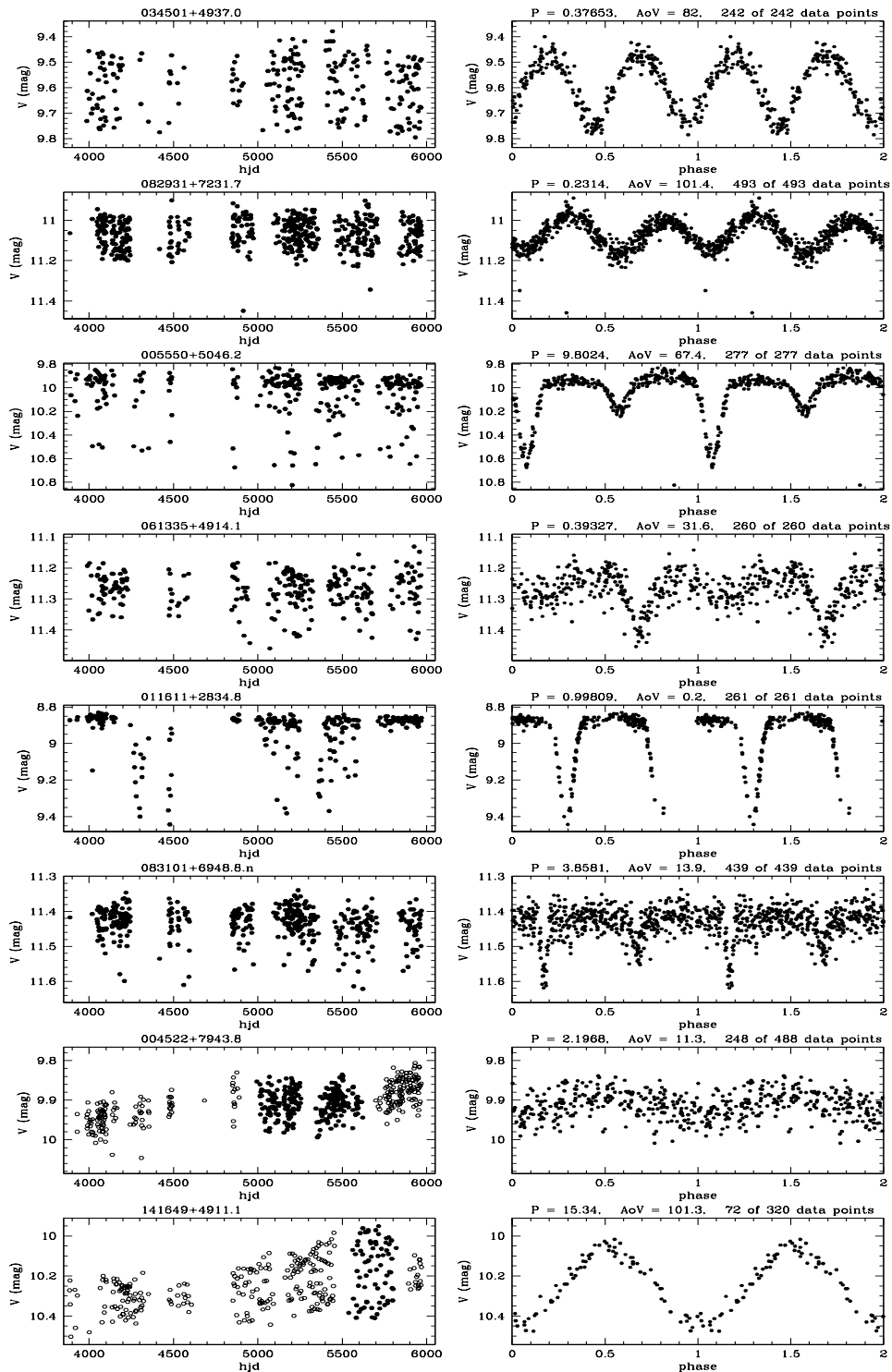


Fig. 5. A few exemplary light curves of the new variables. *Left panels*: V-magnitude vs. hjd = HJD - 2450000, *right panels*: phased light curves. From *top to bottom*: two contact binaries, two β -Lyr type binary stars, two detached binary stars and two spotted rotators.

Table 1
First three entries of Table 1

col. 1	col. 2	col. 3	col. 4	col. 5	col. 6	col. 7	col. 8
1RXS	ASAS	dist	other	name	sp. type	μ_α [mas]	μ_δ [mas]
002116.4+505315	002116+5053.4	11.6	TYC	3259-409-1	~	29.3	-9.2
002415.6+603454	002415+6035.0	7.5	1RXS	J002415.6+603454	~	0.0	0.0
003327.5+575045	003329+5750.6	15.8	1RXS	J003327.5+575045	~	0.0	0.0

col. 9	col. 10	col. 11	col. 12	col. 13	col. 14	col. 15	col. 16
$n(V)$	$\langle V \rangle$	$\sigma(V)$	J	$N_J(40'')$	$F_{J,\text{cor}}(40'')$	J_{cor}	$(V - J_{\text{cor}})$
525	10.139	0.042	8.905	3	1.005	8.900	1.239
276	11.429	0.117	9.772	10	1.192	9.581	1.848
264	11.800	0.049	10.103	7	1.060	10.040	1.760

col. 17	col. 18	col. 19	col. 20	col. 21	col. 22	col. 23	col. 24
cts	err(cts)	HRI	err(HRI)	$\log(F_{\text{bol}})$	R_X	err(R_X)	P [d]
0.070	0.013	0.940	0.120	-8.62	-3.42	0.19	0.862188
0.082	0.015	0.230	0.170	-9.08	-3.03	0.21	0.549447
0.062	0.013	0.730	0.170	-9.21	-2.91	0.22	0.268019

col. 25	col. 26	col. 27
amp	var typ	remarks
0.10	rot	also possible EB/EC and $P = 1.724375$ d
0.37	EB	
0.09	rot	

The consecutive columns of Table 1 contain the following data:

- Column 1 – X-ray source designation from the RBSC catalog (1RXS Jhhmmss.s ± ddmms).
- Column 2 – ASAS designation of the optical ASAS counterpart to the RBSC source (hhmmss ± ddm.m).
- Column 3 – a distance in arc seconds between the position of the ROSAT object and its ASAS counterpart (note that one pixel of the ASAS detector $\approx 15''$).
- Columns 4–5 – another name of the star from the SIMBAD database.
- Column 6 – spectral type from SIMBAD, if available.
- Columns 7 and 8 – μ_α and μ_δ , proper motion in RA, and Dec. [mas/year].
- Column 9 – number of observations in V .
- Columns 10 and 11 – $\langle V \rangle$, mean V -magnitude with uncertainty [mag].
- Column 12 – J -magnitude of the adopted counterpart from the 2MASS catalog.
- Column 13 – number of J -band sources within $40''$ from the ASAS object position.
- Column 14 – the relative total J -flux of all sources counted in column 13 and expressed in units of the flux from column 12.

- Column 15 – J_{cor} , the adopted J -magnitude of the ASAS object.
 Column 16 – color index ($V - J_{\text{cor}}$) (column 10 *minus* column 15).
 Columns 17 and 18 – number of counts per second and its error (RBSC data).
 Columns 19 and 20 – hardness ratio HRI , and its error (RBSC data).
 Column 21 – $\log F_{\text{bol}}$, logarithm of the bolometric flux [ergs/s/cm^2].
 Columns 22 and 23 – R_x , logarithm of the X-ray (0.1–2.4 keV) to the bolometric flux ratio and its error.
 Column 24 – adopted variability period [days].
 Column 25 – maximum amplitude of the V -variability [mag].
 Column 26 – variability type (rot – spotted rotator, ED – detached binary, EB – β Lyr type binary, EC – contact binary, msc – miscellaneous).
 Column 27 – remarks

Table 2

Previously known variable stars with a determined or corrected period

ASAS	other name	new period [d]	old period [d]	remarks and references
005550+5046.2	TYC 3274-955-1	9.80240	1.65977	EB, H09
011611+2834.8	HD 7579	0.998099	–	lt, H31
024242+5027.8	V562 Per	3.98440	–	Hv, P97
033311+1035.9	V1267 Tau	2.113	–	lt, TT*
051111+2813.8	TYC 1858-529-1	2.0141	15.115	lt, TT*, P02
055842-0311.0	ASAS 055842-0311.1	2.202	32.82	P02
065847+2843.0	2E 1751	1.3175	1.6063	H11
110551+5151.3	HI UMa	30.83	11.01	KE02
125533+3011.1	NR Com	5.2109	2.5903	N07
143115+4535.7	EE Boo	49.90	–	Hv, P97
202740+7734.3	BD+77 779	56.80	–	lp, S59
213302+6200.2	V430 Cep	7.771000	–	Hv, P97
230604+6355.6	GJ 9809	2.831000	4.501	KE02

Remarks: lt – long term variability, Hv – unsolved Hipparcos variable, lp – long period variable, EB – β Lyr type eclipsing star, TT* – T Tau type star.

References: H09 – Hoffman *et al.* 2009, H11 – Hartman *et al.* 2011, H31 – Hoffmeister 1931, KE02 – Koen and Eyser 2002, N07 – Norton *et al.* 2007, P02 – Pojmański 2002, P97 – Perryman *et al.* 1997, S59 – Strohmeier 1959.

Variability of thirteen stars listed in our catalog has already been noted in the literature, with periods determined for seven of them. We confirm variability of all of them. They are included into our catalog because we determined variability periods for those six stars with unknown periods and we revised the previously known values for the remaining seven. We also list them separately in Table 2 with additional information.

Very few data exist on parallaxes and/or radial velocity measurements for the investigated stars. We list them in Table 3 with some data repeated from Table 1. It is seen from Table 3 that full kinematic data exist only for seven stars although the value of the parallax for the star ASAS 120216+7221.7 is lower than its uncertainty.

Table 3

List of stars from Table 1 for which kinematical data are available

ASAS	name	μ_α	μ_δ	par.	V_{rad}	P
010122-0519.2	HD 6011	14.18	-8.92	7.83	-	2.11457
021757+3115.8	BD+30 367	-44.1	-53.5	-	27.25	0.310695
022113+4600.1	BD+45 598	44.7	-44.3	-	-0.8	4.729
035720+5051.3	HD 232862	54.9	-75.0	-	-1.80	1.816
051111+2813.8	2MASS J05111053+2813504	4.8	-24.5	-	15.05	2.0141
053139-0327.2	HD 294207	45.2	-52.9	-	27.2	6.642
053704+5231.4	G 191-47	100.90	-208.67	27.61	15.	7.783
093951-2134.3	2MASS J09395143-2134175	-48.1	6.2	-	18.3	0.7952
100228+4434.7	G 146-7	-283.43	-90.17	36.26	30.16	14.92
110551+5151.3	HI UMa	-15.96	-7.69	3.26	-	30.824
120216+7221.7	BD+73 543A	11.48	7.52	0.73	-54.02	7.573
125523+6953.2	BD+70 720	-16.36	-24.94	13.77	-28.1	4.0245
131300+5048.9	LP 132-79	-111.11	95.83	11.12	-	0.38995
134536+6548.2	HD 120163	-28.55	17.51	3.18	-	14.03
143115+4535.7	EE Boo	-53.28	15.24	3.60	-	49.9
150804+6943.9	NLTT 39471	-147.80	77.08	7.36	-	8.628
204128+5725.8	LTT 16050	97.99	206.17	41.26	-	14.118
213240+3604.7	HD 205173	16.6	-1.8	-	-6.2	101.8
213302+6200.2	V430 Cep	371.28	194.39	43.03	-11.14	7.771
221601-1411.0	2MASS J22160063-1411022	50.22	38.71	17.71	-24.4	0.64573
230236+7630.3	HD 218028	151.74	45.91	14.97	-	2.598
230605+6355.6	GJ 9809	171.46	-58.55	40.81	-23.5	2.831
234008-0228.9	BD-03 5686	-34.0	-50.8	-	66.3	2.8968
235451+3831.6	2MASS J3545147+3831363	-130.0	-86.0	-	5.	4.757

Column descriptions: μ_α , μ_δ – proper motion in right ascension and declination [mas/year], par. – heliocentric parallax [mas], V_{rad} – radial velocity [km/s], P – variability period [d]

4. Summary

We present the results of the second part of periodic variability search among stars observed within the photometric survey ASAS and showing a high level of the coronal activity as measured by X-ray flux. This time the Northern part of the survey was analyzed. A catalog with the data on 307 new periodic variables (including a few previously known variables for which the variability period was unknown or in error) is given.

We classified 266 stars as spotted rotators. Among eclipsing stars we found 10 contact binaries, 12 eclipsing binaries with deformed components but not in contact, and 18 detached systems.

Most of the stars have $V - J$ colors and spectral classification consistent with a presence of the outer convection zone and coronal X-ray emission. However, we also identified a few objects with different properties. In particular, the hottest object in the sample is likely a cataclysmic variable, whereas the source of X-ray emission from the reddest star in our list, ASAS 205846+1417.8, is somewhat puzzling. The star may be an M-type giant due to a small proper motion and a large bolometric luminosity, but the stars of this type are not known to be active coronal sources.

Acknowledgements. We are particularly grateful to Prof. Grzegorz Pojmański for help in using ASAS data. This research was partly supported by the National Science Centre under the grant DEC-2011/03/B/ST9/03299. We acknowledge the use of the SIMBAD database, operated at CDS, Strasbourg, France. This publication makes use of data products from the Two Micron All Sky Survey, which is a joint project of the University of Massachusetts and the Infrared Processing and Analysis Center/California Institute of Technology, funded by the National Aeronautics and Space Administration and the National Science Foundation.

REFERENCES

- Casagrande, L., Flynn, Ch., and Bessell, M. 2008, *MNRAS*, **389**, 585.
 Casagrande, L., Ramirez, I., Melendez, J., Bessell, M., and Asplund, M. 2010, *A&A*, **512**, 54.
 Durney, B.R., and Latour, J. 1978, *Geophys. Astrophys. Fluid Dyn.*, **9**, 241.
 Fleming, T.A., Molendi, S., Maccacaro, T., and Wolter, A. 1995, *ApJS*, **99**, 701.
 Hartman, J.D., *et al.* 2011, *AJ*, **141**, 166.
 Hoffman, D.I., Harrison, T.E., and McNamara, B.J. 2009, *AJ*, **138**, 466.
 Hoffmeister, C. 1931, *Astron. Nachr.*, **242**, 129.
 Kiraga, M. 2012, *Acta Astron.*, **62**, 67.
 Kiraga, M., and Stepień, K. 2007, *Acta Astron.*, **57**, 149.
 Koen, C., and Eyler, L. 2002, *MNRAS*, **331**, 45 (KE02).
 Norton, A.J., *et al.* 2007, *A&A*, **467**, 785 (N07).
 Noyes, R.W., Hartmann, L.W., Baliunas, S.L., Duncan, D.K., and Vaughan, A.H. 1984, *ApJ*, **279**, 763.
 Pallavicini, R., Peres, G., Serio, S., Vaiana, G.S., Golub, L., and Rosner, R. 1981, *ApJ*, **247**, 692.
 Parker, E.N. 1955, *ApJ*, **122**, 293.
 Perryman, M.A.C., *et al.* 1997, "The Hipparcos and Tycho catalogues. Astrometric and photometric star catalogues derived from the ESA Hipparcos Space Astrometry Mission", Publisher: Noordwijk, Netherlands: ESA Publications Division, 1997, Series: ESA SP Series vol no: 1200 (Hip).
 Pigulski A., Pojmański G., Pilecki B., and Szczygieł, D.M. 2009, *Acta Astron.*, **59**, 33.
 Pojmański, G. 1997, *Acta Astron.*, **47**, 467.
 Pojmański, G. 2002, *Acta Astron.*, **52**, 397 (P02).
 Pojmański, G. 2004, *Astron. Nachr.*, **325**, 553.
 Roberts, D.H., Lehar, J., and Dreher, J.W. 1987, *AJ*, **93**, 968 (CLEAN).

- Schwarzenberg-Czerny, A., 1989, *MNRAS*, **241**, 153 (AoV).
Skrutskie, M.F., *et al.* 2006, *AJ*, **131**, 1163.
Soszyński I., *et al.* 2011, *Acta Astron.*, **61**, 217.
Strohmeier, W. 1959, *Astron. Nachr.*, **285**, 87 (S59).
Voges, W., *et al.* 1999, *A&A*, **349**, 389.
Wilson, O.C. 1963, *ApJ*, **138**, 832.